MINERALOGICAL MAGAZINE

JOURNAL OF THE MINERALOGICAL SOCIETY

Vol. 35 December 1966 No. 276

The petrology of the Mount Padbury mesosiderite and its achondrite enclaves

By G. J. H. McCall[1]

(with chemical analyses by H. B. Wiik[2] and A. A. Moss[3])

[Taken as read 3 November 1966]

Summary. The petrography of the Mount Padbury meteorite, previously briefly recorded, is described in some detail. Both the metalliferous host material of the mesosiderite and the varied range of silicate-rich, virtually metal-free enclaves (including both familiar achondrite material and unfamiliar achondrite material) are described. Eucrite, brecciated eucrite, and a peculiar 'shocked' form of eucrite (resembling some terrestrial *flaser-gabbros*) are the calcium-rich achondrite types represented; hypersthene achondrite (including typical diogenite material and unfamiliar material) and olivine achondrite (granular aggregates of olivine not entirely similar to the unique chassignite and single crystals up to 4 in. in length) are the calcium-poor achondrite types represented. The eucrite displays more or less uniform mineralogy, but the mineral constituents are present in varying proportions, and there is a wide range of textural variations recognized. The silicate grain fragments enclosed in the metallic reticulation to form the mesosiderite host material are, significantly, entirely of minerals seen within the achondrite enclaves—plagioclase, hypersthene, pigeonite, olivine, and tridymite.

These results include microscopic analysis of thin sections and polished sections, X-ray diffraction studies, optical determination of refractive indices using mineral grain mounts, and chemical analyses.

The wider implications of this new and unique meteorite find are briefly considered.

McCALL and Cleverly (1965) have recently furnished a brief account of the discovery of this stony-iron meteorite on Mt. Padbury sheep station, Western Australia (25° 42′ S, 118° 15′ E (fig. 1)). The find was made on 12 March 1964 by one of the joint managers of the station, Mr. W. C. Martin, while mustering sheep. Initial mention of the new find had previously been made by McCall (1965*a*) and McCall and de Laeter (1965). Cleverly (1965) has, in a separate publication, covered

[1] University of Western Australia, Geology Department. Honorary Associate, Western Australian Museum.

[2] Arizona State University, Tempe, Arizona, Department of Chemistry.

[3] British Museum (Natural History), Department of Mineralogy.

the details of the recovery by himself of more than 600 lb of fragments, noting their distribution on the ground and other relevant details. From this material, brought back by Cleverly and kindly made available, the writer has been able to select certain fresh material for megascopic, microscopic, and chemical analysis.

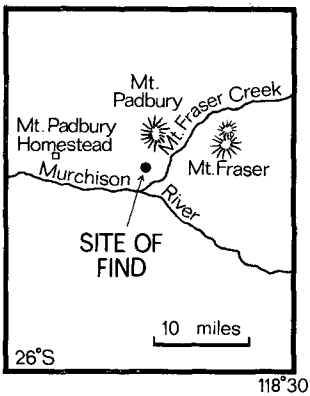

FIG. 1. Sketch map showing the location of the find.

The material selected does not, it is emphasized, cover the whole store of meteoritic material from Mt. Padbury held in this State, both in the collections of the School of Mines, Kalgoorlie, and in those of the Western Australian Museum, Perth. Two of the largest fragments held in the former collection (Cleverly, 1965) have not, as yet, even been cut because of technical difficulties.

The material selected for study comprises: A single mass, weight 25 lb, entirely fresh throughout and covered only by a thin film of iron oxides (fig. 2); another large mass, weight 70 lb, this mass has only been studied in polished face and exterior surface, with the exception of one prominent eucrite enclave (Figs. 3 and 5); a small faceted fragment, completely fresh (fig. 4); various small lumps of mesosiderite displaying achondrite enclaves (*e.g.* fig. 6) and also various detached fragments entirely composed of achondrite material—fragments found quite isolated from the mesosiderite host material which, presumably, once enclosed them (figs. 7 and 8); and several large olivine crystals recovered separately from the mesosiderite host material or else mechanically removed from it (fig. 9).

External features. Cleverly (1965) has adequately covered the external features of the meteorite fragments and little need be added here. However, since that account was published certain small fragments possessing angular, indented facets have been noticed and the question whether such fragments represent individual masses that arrived quite separated from the larger fragments is discussed. One such fragment is illustrated in fig. 4: 3 in. in length, it shows a smooth, convex face on one side, but indentations very like those illustrated by Krinov (1961, p. 234; fig. 80) appear on the other face. Such indentations are *not* classified by Krinov as true rhegmaglypts, and, indeed comparison of

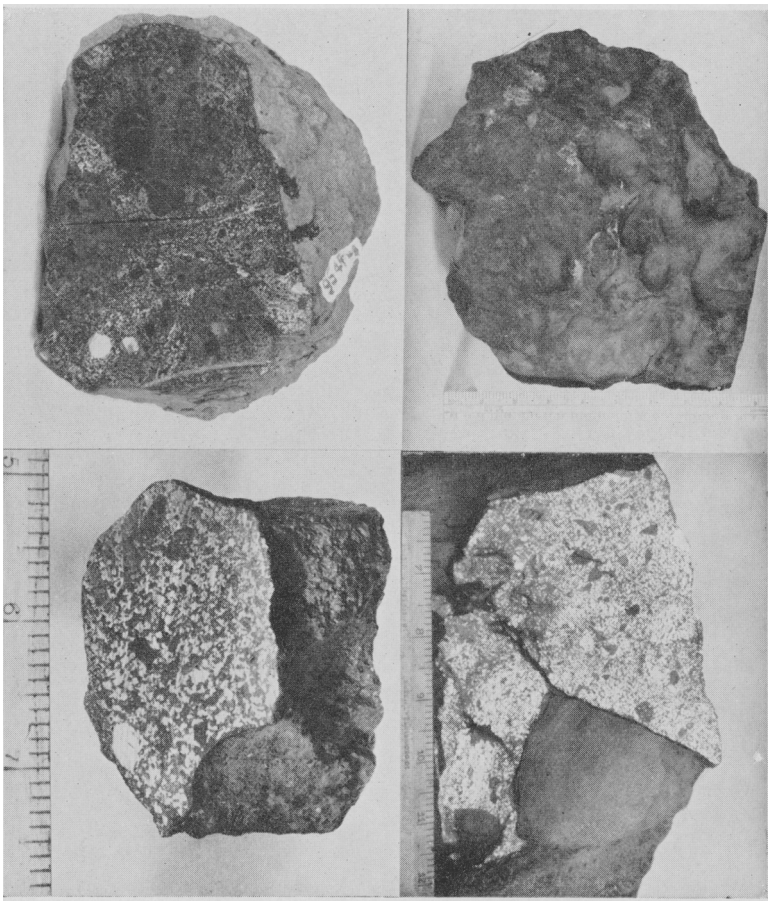

FIGS. 2–5 (scales in inches): FIG. 2 (top left). A 25-lb fragment, showing cut face, in which fresh mesosiderite material forms a metalliferous host enclosing achondritic enclaves and metallic nodules ($\times 0{\cdot}4$). FIG. 3 (top right). A primary ablation surface; 70-lb fragment. FIG. 4 (bottom left). A small faceted fragment; the hollowed-out facets are probably due to secondary atmospheric ablation. The cut and polished face shows the fresh nature of the material, the fine mesosiderite network texture of the host material and inset areas formed by achondrite enclaves and metallic nodules. FIG. 5 (bottom right). Cut face of the 70-lb fragment shown in Fig. 3. The mesosiderite host material encloses numerous achondritic enclaves; a particularly large eucrite enclave (> 3 in. across) is separated from another such enclave beneath it by a very narrow isthmus of host material. The angular form of the enclaves is clearly seen, as is their ready detachment from the host material.

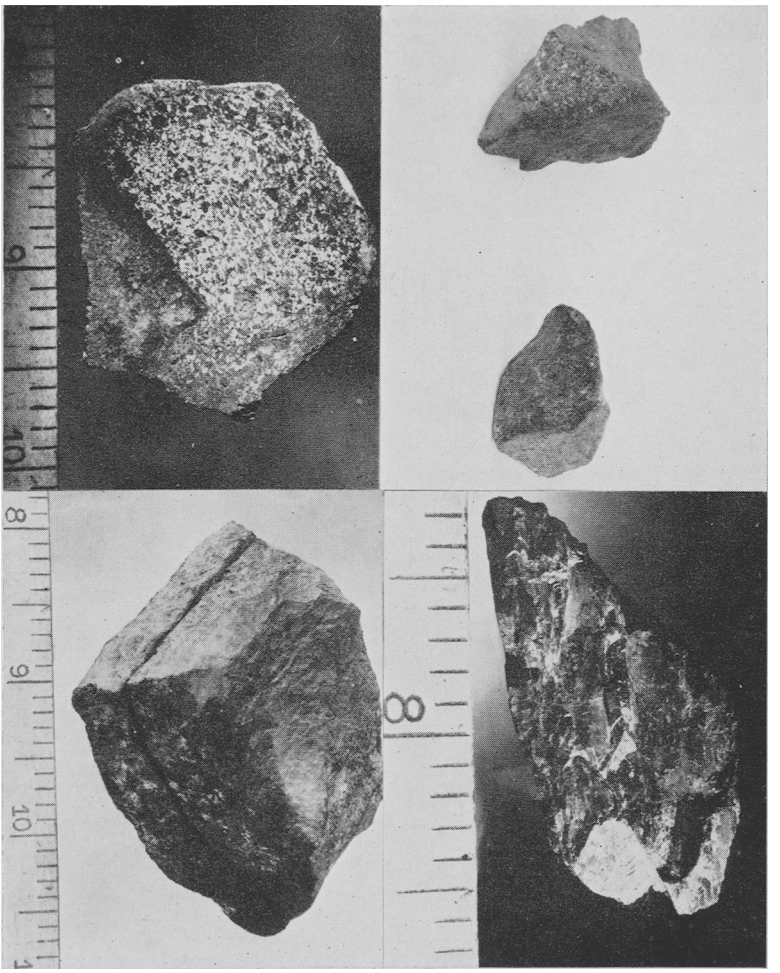

FIGS. 6–9 (scales in inches): FIG. 6 (top left). A small fragment showing an angular eucrite enclave, bordered by a zone of discoloration due, probably, to contact metamorphism. FIG. 7 (top right). Two small, angular fragments of eucrite, recovered detached from the host material ($\times 0{\cdot}5$). FIG. 8 (bottom left). The large eucrite enclave shown in Fig. 5, detached from the host material enclosing it: the faceted angular form and fresh surface is clearly seen. FIG. 9 (bottom right). Olivine crystal recovered detached from the host material. The cross-cleavages are prominent.

these indentations with those on the surfaces of the larger Mt. Padbury masses (fig. 3) suggest that they are not, like them, surfaces of the 'first kind', primary ablation markings (Krinov, 1961, p. 190). They are thus considered to be ablation markings on surfaces only exposed to ablation by the effect of fragmentation at a late stage in atmospheric flight—secondary ablation markings. These fragments would, therefore, have arrived as separate masses, but have undergone separation from the larger masses at no great altitude above the surface of the earth.

Megascopic details. The polished surface of a cut section from the mass illustrated in fig. 2 reveals a characteristic mesosiderite texture (fig. 10), and similar texture is revealed by other cut sections (figs. 2, 4, 5, and 6). Mesosiderites are characterized by finer textures than the pallasites and lodranites, or than the anomalous Bencubbin meteorite (Lovering, 1962: McCall and de Laeter, 1965), an enstatite-bearing stony-iron. The fine nickel-iron reticulation of the Mt. Padbury mesosiderite is in every way typical of the 'true mesosiderite' (McCall, 1965*b*). It is mostly composed of a single phase, no pattern being obtained on etching with nitric acid except in the case of some metallic nodules; the latter produced a Widmanstätten pattern and the fineness of kamacite lamellae (av. width 0·5 mm) requires classification on the very border line between fine and medium octahedrites (Of–Om). The pattern is very similar to that shown by metallic nodules from the Dalgaranga mesosiderite (Nininger and Huss, 1960, p. 631, fig. 9), there being a swathing envelope of kamacite. Such scattered, ganglion-like nodules of continuous metal (figs. 2, 4, and 10) are apparent in all true mesosiderites.

Troilite is approximately one-quarter as abundant as nickel-iron in the mesosiderite material and is not to any appreciable extent aggregated with the metal phase, being finely interlaced with the silicate mineral fragments, which are themselves enclosed in compartments within the nickel-iron reticulation (fig. 12). This distinct separation of metallic and sulphide phase (also noted in Bencubbin) has not, perhaps, been fully considered with respect to possible genetic implications.

The metal-free areas within the metallic mesh work are of varied composition. The small reticulations are occupied by silicate grains and microscopic lithic fragments, the reticulations averaging half a millimetre in diameter. These silicate enclosures have the form of a breccia. In contrast, the larger, sporadic areas of silicate (figs. 2 and 5) are either composed of single crystals of olivine or granular aggregates of virtually metal-free, achondritic material. The specific achondrite type is not

usually recognizable without the aid of a microscope, on account of the fineness of texture. These achondrite enclaves and the single olivine crystal insets tend to be fringed by haloes showing enhanced coarseness of nickel-iron crystallization, but this effect is by no means universally apparent.

The included olivine masses display an oily lustre and light brown surfaces, showing iridescence. In colour they are lighter than the majority of the eucrite enclaves, which do not present such extensive crystal cleavage faces manifesting iridescence. The eucrite inclusions are rarely sufficiently coarsely crystalline to reveal their ophitic texture clearly to the naked eye, though they usually appear finely speckled due to the contrast of feldspar and pyroxene. The diogenite enclaves reveal the brownish, slightly oily colouration typical of many terrestrial hypersthenites, and may show glistening 'phenocrysts', standing out from the finer, granular matrix when the cut face is seen under certain conditions of illumination.

A conspicuous feature of the achondrite enclaves is their angularity (figs. 5, 6, 7, 8, and 9), which is more consistently developed in the larger enclaves and not so apparent in the smaller ones, some of which may even show rounded outlines (figs. 2 and 5).

A distinct marginal zone of staining circumscribes one prominent enclave, while the host material enclosing it is quite unchanged up to the contact (fig. 6). This phenomenon suggests invasion of the enclaves by the metallic melt and not the converse—the same deduction can, of course, be made on account of the occurrence of the achondrite material only as islands within an extensive mass of continuous metalliferous host material; the lack of inclusion of metallic material in the achondrite material and lack of veining or digitation of the metallic material by achondrite material is surely conclusive evidence on this point. Yet in spite of this conclusion it must be remarked that the achondrite enclaves are surprisingly little penetrated by the metal: there seems to be an abrupt cut off to the nickel-iron penetration once one reaches the interface, the boundary of the solid, virtually unbrecciated achondrite masses, which predominate and contrast with the brecciated silicate of the reticulations within the host material. In a few cases specks of nickel-iron have been recognized on cut surfaces of achondrite enclaves, well beyond the interface and entirely enclosed in eucrite: there is also limited penetration of nickel-iron down fine cracks, which mark incipient brecciation, and traces of nickel-iron, highly reflectant, are aggregated with the primary ore (mostly magnetite) in some achondrite enclaves.

Specific gravity. Determinations have been carried out on two fragments of the mesosiderite host material, relatively fresh material devoid of substantial enclaves (such as is shown in fig. 4). Values of 4·22 and 4·46 were obtained, and the latter figure, taken on the actual piece used for chemical analysis, indicates 56 % by weight of metal, 44 % by weight of silicate, a value not in conflict with modal estimation of

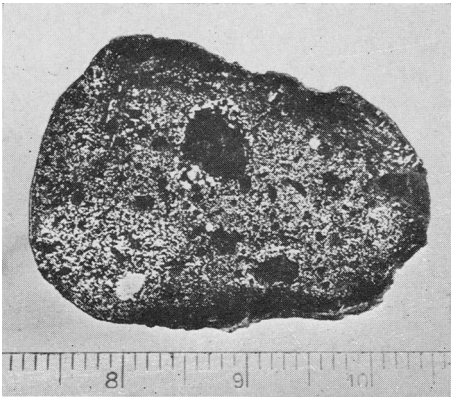

FIG. 10. Cut and polished section taken from the mass shown in Fig. 2, showing the fringing 'wall' of coarse metal crystallization surrounding some achondritic enclaves.

these fractions, though this material is so variable texturally that any modal or chemical analysis only refers to a particular sample selected; another such sample would, in all probability, yield quite different values. It is certainly evident that the silicate is slightly subordinate to the nickel-iron throughout the meteorite. Determinations on eucrite enclaves yielded values of 3·16 and 3·18 on two selected specimens. Such values are typical of eucrites (av. 3·23, Wood, 1963, p. 342), though rather higher than the expected value for terrestrial igneous rock of like composition—for example, quartz dolerite (diabase) has an average specific gravity of 2·965 according to Clarke and Washington. This deviation is interesting and unexpected for quartz has a higher specific gravity than tridymite, present in this eucritic material (quartz, 2·65; tridymite, 2·26). The eucrite may be expected to show slight variation of density, reflecting the variations in mineralogical composition evident in thin section.

A single diogenite enclave yielded a sp. gr. of 3·45, closely matching the values obtained for the known members of this rare meteorite group —3·37, 3·40, 3·40, 3·41, and 3·41 (Mason, 1963, p. 9). A single olivine achondrite enclave yielded a value of 3·37.

Microscopic details of the host material. In thin section the host material is seen to include numerous grains of pigeonite showing pronounced exsolution lamellae, less abundant grains of hypersthene and very sparse grains of olivine, which are, however, of somewhat larger size than the other ferromagnesian mineral grains. Plagioclase (bytownite) is abundant, but tridymite is rarely recognizable. The olivine is mostly present as single isolated crystals, but the pyroxene and feldspar may be aggregated in composite fragments, some of which amount to minute lithic inclusions of eucritic or other achondritic material.

Many of the included silicate grains within the continuous opaque nickel-iron meshwork appear broken, showing irregular form (fig. 13). The size of the pyroxene and feldspar grains is variable and there seem to be two distinct generations reflected in larger grains averaging $0{\cdot}5 \times 1{\cdot}0$ mm and smaller grains averaging 0·1 mm maximum diameter, the two generations being separated by a distinct hiatus. Some of the larger pyroxene grains evince skeletal form, especially pigeonite—a feature which seems to be due to partial incorporation in the fine groundmass rather than incomplete initial crystallization. There could be some relationship between this effect and the fine granulation of some eucrite enclaves.

The silicate grains are only of minerals characteristic of the eucrite, hypersthene achondrite, and olivine achondrite enclaves described below—a fact that seems highly significant. The composite aggregates of grains (or minute lithic inclusions) are mostly of a character compatible with derivation from break up of the achondrite types represented in the enclaves. An exception to this is a very small lithic inclusion of a type only known from this particular minute lithic fragment, the inclusion composed of finely lamellated pyroxene illustrated in fig. 32 and further described on p. 1053. A lithic inclusion composed of a fine aggregate of equigranular, lamellar-twinned calcic plagioclase is clearly derived from the type of 'shocked' eucrite enclave described on p. 1049 below (and illustrated in fig. 24). This occurrence clearly establishes the fact that this 'shock' granulation took place before the invasion of the nickel-iron and the brecciation that accompanied it.

Some lithic inclusions show incipient fragmentation (fig. 32), the sutures between the grains being infilled with ferruginous material and

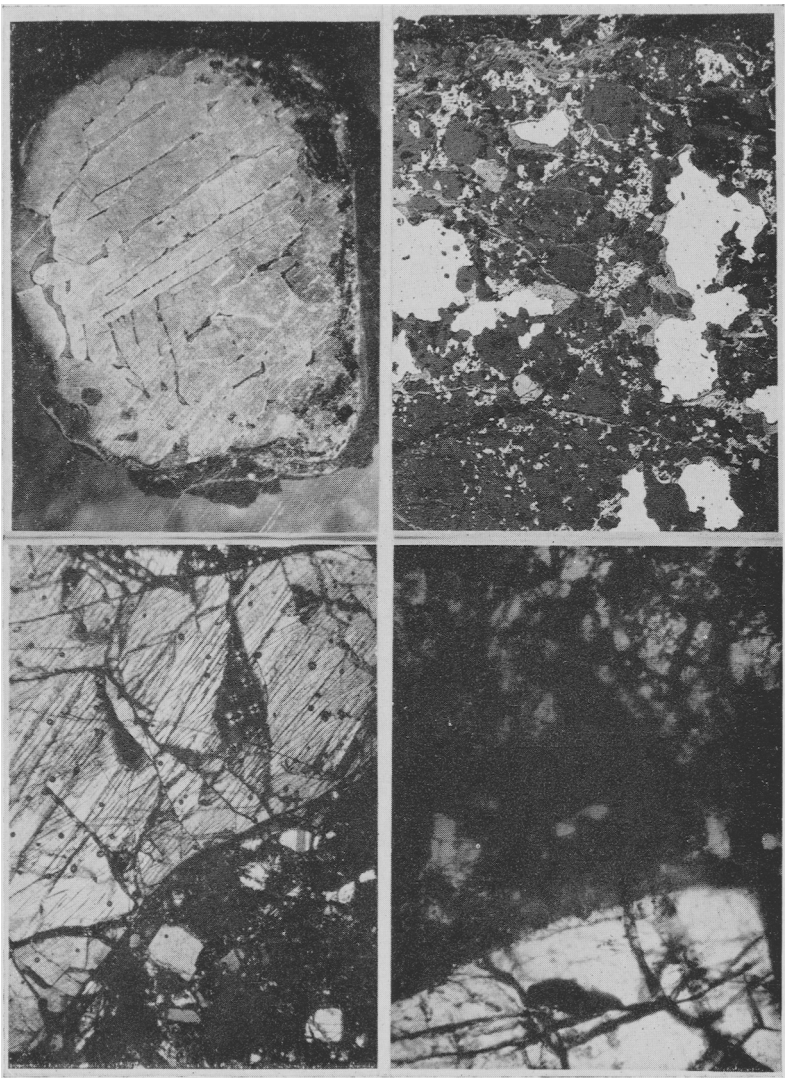

FIGS. 11–14: FIG. 11 (top left). Cut and polished surface of a metallic nodule showing the Widmanstätten pattern developed by etching with nitric acid ($\times 6$, reflected light). FIG. 12 (top right). Polished section of the host material: nickel-iron (white); troilite (bright grey); silicates (dark grey); iron oxides (medium grey). The clear-cut separation of troilite and nickel-iron is well displayed ($\times 21$, reflected light). FIG. 13 (bottom left). (W.A.M. 12297 1): A large olivine crystal inset in the host material; angular fragments of bytownite, showing polysynthetic twinning, and pyroxene, showing light grey, are set in a metallic base (opaque) ($\times 15$, crossed nicols). FIG. 14 (bottom right). (W.A.M. 12297 1): Another such olivine crystal; a cryptocrystalline selvedge is apparent and suggests contact fusion of the olivine at the margin ($\times 38$; plane polarized light).

the grains slightly moved apart by the opening up of these sutures. Such ferruginous intergranular filling material is mostly converted to oxides, though some primary metal is occasionally preserved.

One of the larger included olivine grains displays a halo of cryptocrystalline, metal-free material (fig. 14): this suggests fusion at the margin by the agency of the invading metalliferous melt. Whether this interpretation is correct or not this textural relationship seems difficult to reconcile with anything but the incorporation of pre-existing olivine crystals within the metallic fraction, a relationship established in the case of the Dalgaranga mesosiderite (McCall, 1965*b*).

Separation of the silicate grains from the host material has allowed exact identification of the following mineralogical species by refractive indices determination in oils (using sodium light): Pigeonite, α 1·703, γ 1·733, 2V small, giving a composition $Wo_{12}En_{45}Fs_{43}$; hypersthene, γ 1·698, giving Fs_{28}; plagioclase, γ 1·579, giving An_{85}; olivine, α 1·645, γ 1·686, giving Fa_8.

Tridymite is also present and is identical in appearance with that separated from the achondrite enclaves (p. 1045).

Microscopic details of the inclusions

Olivine achondrite inclusions. Occurring mostly in the form of large, isolated olivine crystals, up to 4 in. in length (fig. 9) and as aggregates of olivine grains, the olivine achondrite enclaves grade insensibly into large, sparse, isolated olivine crystals within the host material (fig. 14). All appear to be of the same composition. Grains obtained by crushing part of one of the large isolated crystal enclaves were found to have α 1·645, γ 1·686, corresponding to Fa_8. X-ray diffraction study (utilizing the method of Yoder and Sahama, 1957) gave a value of Fa_9 for the same material and this value (determined by Dr. Mason together with the refractive indices) is taken as correct. It corresponds to the extreme magnesian variety of olivine so far recognized in mesosiderites, but is a value that has now been recognized in no less than four mesosiderites (McCall, 1965*b*, p. 484, Table 1). As in all true mesosiderites (McCall, 1965*b*, p. 484) this value shows no agreement with the ferrosilite indices obtained for the hypersthene in the host material (Fs_{28}). Both values are, however, within the ranges reported for mesosiderites, and the hiatus separating them is of a typical order of magnitude.

The olivine shows unusually good cleavage—so good that it seems anomalous. It is developed on (010) and (100), and is not easy to distinguish from the cleavage of the hypersthene (as in the diogenite

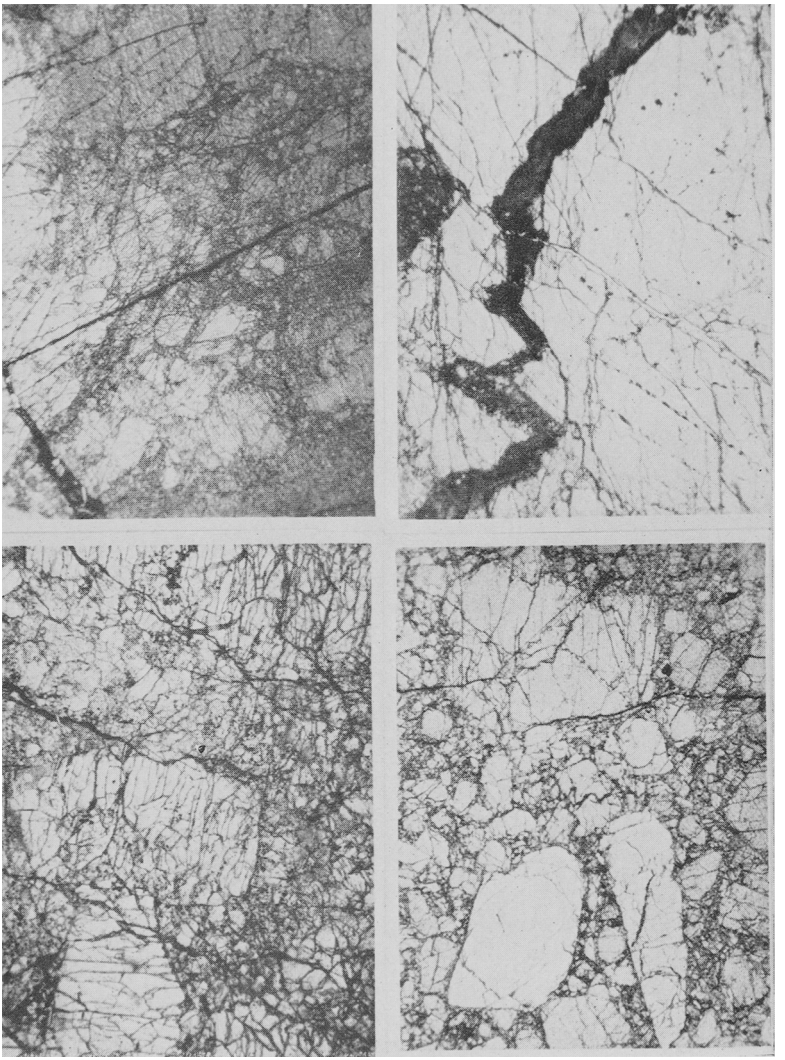

FIGS. 15–18: FIG. 15 (top left). (W.A.M. 12297 hh): Olivine achondrite enclave, showing brecciated texture and narrow, dark veinlets of fine crush material ($\times 6$; plane polarized light). FIG. 16 (top right). (W.A.M. 12297 hh): Olivine achondrite enclave, showing the fine-crush veinlets under higher magnification ($\times 15$; plane polarized light). FIG. 17 (bottom left). (W.A.M. 12257 hh): Olivine achondrite enclave, showing the remains of an original medium-coarse, granular texture, now partly obliterated by intergranular comminution. The anomalously good cleavage of the olivine is apparent ($\times 37$; plane polarized light). FIG. 18 (bottom right). (W.A.M. 12297 cc): Olivine achondrite enclave, showing a type of brecciation texture characteristic of many stony meteorites. In spite of the intergranular comminution, one olivine grain has preserved euhedral form. The cleavage again appears anomalously good ($\times 6$; plane polarized light).

enclaves for example, figs. 30 and 31). However, the cleavage of the pyroxene is more perfectly 'ruled' and that of the olivine is less perfect, often appearing slightly sinuous (fig. 17), and the olivine has a positive, not a negative, optic sign.

While large single crystals predominate, composite enclaves are not rare; these clearly derive from brecciation of crystalline, granoblastic aggregates of substantial olivine crystals, identical in composition with the single crystals. The textural evidence shown in figs. 15, 16, 17, and 18 clearly establishes the fact that the granulation and brecciation affected aggregates of grains in diverse orientation, not just single crystals. In the enclaves shown in figs. 15, 16, and 17 the granulation has been patchy, leaving a rather irregular porphyroclastic texture, but in that shown in fig. 18 there is an even grain-boundary granulation producing a type of brecciation texture familiar in stony meteorites. In fig. 16 we see evidence of the formation of finely crushed material, appearing cryptocrystalline, in a series of narrow veinlets. This fine crush is composed of grains showing second order polarization colours and positive relief, often appearing fibrous. It may be nothing more than finely crushed olivine.

Specks of metal and troilite can be recognized within these veinlets and the possibility is suggested that these crush veinlets reflect the brecciation phase that accompanied the nickel-iron invasion responsible for the metallic network of the host mesosiderite material. In one such enclave veinlets of crush are observed to transect brecciated material (like that shown in fig. 18) sharply (fig. 15), indicating a prior brecciation phase and a subsequent phase of brecciation involving fine-crush veining and metallic invasion. Yet it must be remarked that in yet another instance nickel-iron and troilite seem to have entered the olivine achondrite along narrrow zones of granulation of the olivine (fig. 18). The inference is drawn that crystal-boundary granulation and subsequent fine crush veining represent phases of deformation not long separated in time—early and late stages of a process that modified an aggregate of inhomogeneous stony (achondritic) material to its present stony-iron character. The olivine inclusions show no significant metallic or silicate constituent minerals other than those evident in the zones of granulation or fine crushing. They are thus achondrite enclaves of virtually monomineralic character—the only material other than olivine so far recognized is in the form of dark specks that dust the interior of the olivine.

X-ray diffraction determination by J. R. de Laeter of the olivine in the granulated enclave 'N' (figs. 15, 16, and 17) gave a value of Fa_9 for

the olivine, identical with the value obtained for single crystal enclaves.

The olivine is quite different from that present in the unique chassignite (Fa_{33}: Mason, 1962, p. 111), there is no chromite or plagioclase so far detected and the texture is very different, the chassignite appearing megascopically much more like a terrestrial dunite. The name chassignite is thus not applicable to these enclaves.

The eucrite[1] *inclusions* might well be taken for individual stony meteorites if found entirely separated from the mesosiderite host material by the agency of impact fragmentation or late atmospheric fragmentation. Indeed, it is not improbable that some indication of association might be revealed by a study of geographical distribution of the mesosiderites, eucrites, howardites (and even the diogenites). The angularity of the enclaves, which separate readily from the host mesosiderite material, coming away as angular stones bounded by fresh, faceted surfaces (figs. 7 and 8), suggests invasion by nickel-iron of a fractured mass of heterogeneous achondrite material of predominantly eucrite composition. The fact that some enclaves are embayed by nickel-iron and silicate fragments (the host material) along minor fracture planes, and that some adjacent eucrite enclaves are separated from one another by only a narrow isthmus of host material and reveal identical petrographic characteristics, supports this interpretation (figs. 2, 5, and 19).

While there is evidence of genetic connexion between eucrite and diogenite enclaves (p. 1055), no evidence of such a connexion has been found in respect of the olivine achondrite enclaves described above and the eucrite. The three types are only found as discrete masses, and neither of the calcium-poor achondrite types has, in fact, been found included within the eucrite (the evidence of the diogenite–eucrite relationship depends on the sharing of interstitial tridymite of identical character). Yet we must bear in mind the olivine–howardite relationship observed in Dalgaranga (McCall, 1965*b*), and expect similar composite achondrite enclaves to be eventually recovered in the case of Mt. Padbury. The lack of such recovery is probably due to the mechanical weakness of the plane bounding areas of different achondrite types within the silicate mass prior to nickel-iron invasion, separation and intrusion

[1] The terms eucrite and howardite are used by the writer as redefined by Mason (1962, pp. 113–114)—there are other usages. The Mt. Padbury enclaves are eucritic since clinopyroxene is exclusively present or dominant, not hypersthene as in the Dalgaranga howardite enclosure (McCall, 1965*b*).

almost always occurring along these boundaries. The eucrite is certainly never found enclosed within the olivine enclaves, the converse relationship—a significant fact.

The eucrite inclusions are numerous and varied in texture and composition. A number of examples are described below, and the various specimens are connected by letter suffixes to the Western Australian

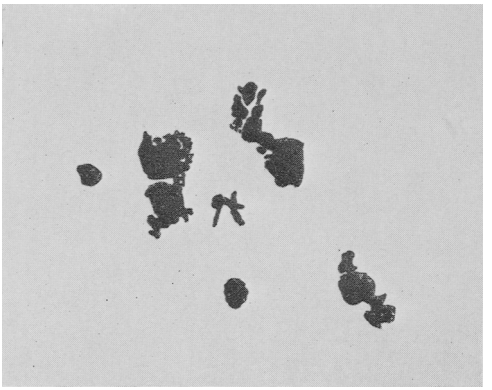

FIG. 19. Diagram showing the textural relationships of some achondritic enclaves to the host material and to one another. Enclaves are shown dark: host material colourless ($\times \frac{3}{4}$).

Museum No. 12297 (given to the entire Mt. Padbury representation in that collection). It will be noted that textural variations outweigh compositional variations, and that these textural variations are either primary (textures formed at the time of initial crystallization, including ophitic, sub-ophitic (passing to intergranular), and granulitic) or secondary (textures imposed by subsequent deformation, including 'shocked' and brecciated textures).

Of the *primary* textures any one may grade insensibly into another. The ophitic texture is characterized by plagioclase laths interdigitating with and entirely enclosed by pyroxene granules (fig. 20). Similar interdigitation characterizes the sub-ophitic texture (figs. 21, 22) but the granules form islands enclosed by a continuous area of feldspar laths. In some cases the elongation of the feldspar becomes very weakly developed and thus leads to a gradation into granulitic textures, which neither show elongation nor interdigitation (fig. 23): in these textures both pyroxenes and feldspars form an equigranular mosaic of rounded grains, such as is characteristic of terrestrial metamorphic granulites.

The sub-ophitic texture may, alternatively, grade into intergranular texture, due to elongation of the feldspar laths and enclosure of the pyroxene in the triangles and polygons between the meshing laths (fig. 29).

The *secondary* textural variants include the shocked type in which constituent minerals have been converted to finely granular aggregates of the same mineral, while retaining their outlines (fig. 24), and the brecciated type in which there has been rupture and comminution to impose a completely new texture, and to develop an aggregate of angular fragments and fine crush.

Enclave F is characterized by a *sub-ophitic* texture, in which elongation of the feldspars is slight and the constituent grains are almost equidimensional; areas of the thin section approach granulitic texture. Megascopically the enclave appears finely granular, phaneritic, free of nickel-iron, and light brown in colour. Like all the other eucrite enclaves studied in thin section, it stems from a fragment recovered entirely detached from the metallic host material.

Broad laths of bytownite plagioclase (An_{77}) up to 1·55 mm long digitate into equidimensional grains of pigeonite (up to 0·55 mm), aggregated interstitially to the continuous feldspar aggregate (fig. 21). The feldspars are subhedral, the pigeonite anhedral. The former show turbid areas devoid of cleavage and water-clear areas manifesting good cleavage: the turbid areas are seen under high magnification to be riddled with droplet inclusions coloured pale pink, pale violet, or bluish grey (fig. 22). These inclusions are commonly aligned to form trains of spindles and rounded droplets parallel to the cleavage planes of the host crystal (fig. 22). The clear and turbid areas are not arranged in any regular zonation pattern—one end of a particular individual bytownite lath may be turbid, the other clear and inclusion free. There does, however, appear to be a tendency for the clear areas to enclose turbid areas rather than the converse. This 'droplet-inclusion' phenomenon is already recorded from the Moore County eucrite (Hess and Henderson, 1949). The feldspar is well twinned, and shows some anomalous twinning, apparently a stepped type of pericline twinning. The feldspar, like the other minerals, shows no trace of alteration.

The pyroxene is pigeonite, characterized by moderate birefringence, oblique extinction, low optic angle ($2V \sim 10°$) and prominent exsolution lamellae (? of augite). There are two types of lamellar structure evident: broad prominent lamellae due to twinning on (100), and fine lamellar structure due to exsolution of augite parallel to (001). Both

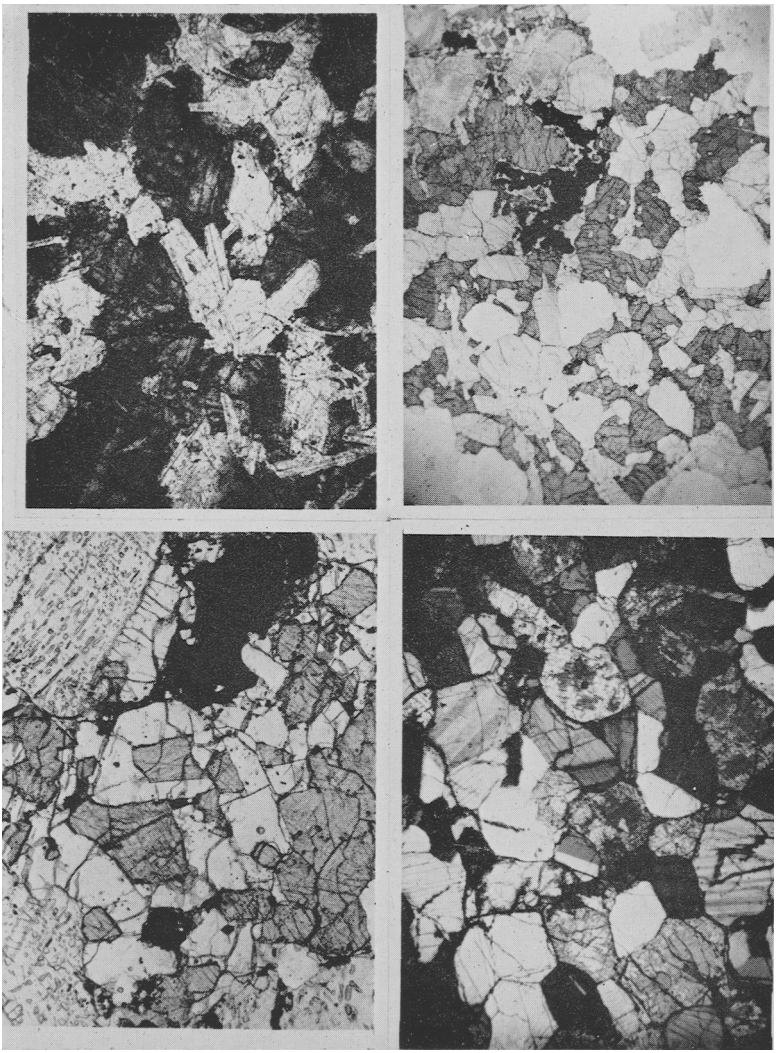

FIGS. 20–23: FIG. 20 (top left). (W.A.M. 12297 z): Eucrite enclave showing ophitic texture; bytownite (white); pigeonite (dark) ($\times 37$; plane polarized light). FIG. 21 (top right). (W.A.M. 12297 q): Eucrite enclave showing sub-ophitic texture: bytownite (white); pigeonite (grey); tridymite (minute white specks); and ore mineral, magnetite aggregated with a few specks of nickel-iron (?) (black) ($\times 6$; plane polarized light). FIG. 22 (bottom left). (W.A.M. 12297 p): Eucrite enclave showing tridymite (white) intergrown with pigeonite (grey). The U-shape of some tridymite grains is apparent. Bytownite (off-white, with many bubble-like inclusions following cleavage directions), and ore minerals (black) make up the

these lamellation structures are seen in all the eucrite enclaves studied. Hypersthene could not be detected.

Tridymite is prominent in the form of small, colourless grains (fig. 22), showing straight extinction to the elongation, and biaxial positive interference figures with moderate optic angles (2V $\sim 60°$). The appearance of these grains is mottled under crossed nicols, in shades of grey, the birefringence being extremely weak ($\sim 0{\cdot}003$). The mottling appears to be due to sector twinning, which is locally quite regularly defined. Simple twinning parallel to the length of the grains is also evident. The elongation is negative. Some grains are of irregular shape, and U-shaped grains are not uncommon (fig. 22). The tridymite is commonly aggregated with pyroxene and ore minerals, but seldom with bytownite and seldom is it enclosed in it.

The ore mineral is predominantly magnetite but some highly reflectant specks in it may be nickel-iron. In the subsequent descriptions the ore is referred to as magnetite though there may be minor associations of other opaque minerals with it—the greater part has the reflectance of magnetite.

The mode is: Bytownite 44·5 vol. %, pigeonite 46, tridymite 3, magnetite 6·5. This particular enclave cannot represent anything but material crystallized from a melt of predominantly silicate composition magmatic material. This is true of all the eucrite enclaves—ophitic textures cannot be produced in any other way, as far as is known, and the enclaves devoid of ophitic textures show the same crystallization sequence. In this case the texture indicates initial crystallization of plagioclase with pigeonite soon coming out of solution with it. Tridymite came out late as an end-phase and magnetite even later.

Enclave G shows a truly ophitic texture, the feldspar being set in a continuous aggregate of pyroxene granules. The feldspar is bytownite (An_{80-84}). The pyroxene is pigeonite (2V ~ 0) and some of the tridymite grains are excessively long and attenuated (up to 5 mm). A network of fine cracks testifies to incipient break-up: they are infilled with nickel-iron, troilite, and iron oxides. The mode is: Bytownite 34 vol. %, pigeonite 59½, tridymite 4½, magnetite 2. The crystallization has

remainder of the photograph ($\times 37$; plane polarized light). FIG. 23 (bottom right). (W.A.M. 12297 r): Eucrite enclave showing granulitic texture: bytownite (white, and showing polysynthetic twinning); pyroxene (zoned in shades of grey; outer zones are hypersthene and inner zones pigeonite); and tridymite (small interstitial grains, mottled grey (half way up, extreme right). The characteristic intergranular growth of the tridymite is clearly seen (*cf.* Fig. 32) ($\times 15$; crossed nicols).

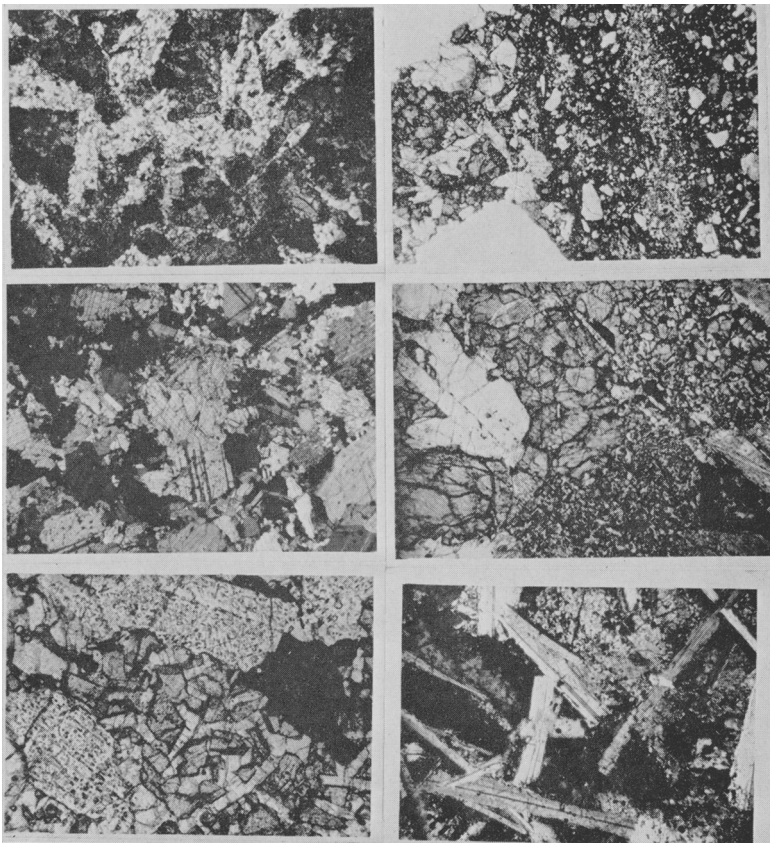

FIGS. 24–29: Fig. 24 (top left). (W.A.M. 12297 w): shocked eucrite enclave showing relict ophitic texture. Plagioclase laths (white) have suffered intense granulation and recrystallization; pigeonite (dark) shows only some marginal granulation and recrystallization (×11; plane polarized light). FIG. 25 (top right). (W.A.M. 12297 v): brecciated eucrite showing an unbrecciated eucrite residual (right) and bands of truly brecciated material, consisting of angular fragments of the silicate minerals of the eucrite. The narrow, light-coloured band is shot through with specks of nickel-iron; the remainder is not (×4; plane polarized light). FIG. 26 (middle left). (W.A.M. 12297 o): eucrite showing a texture gradational between the sub-ophitic and granulitic types. The lamellar twinning of the bytownite (light area) and the broad, stubby character of the feldspar laths is apparent. Pigeonite grains (grey: upper, extreme right) show lamellar twinning parallel to (100) and an oblique lamination due to exsolution parallel to (001) (×11; crossed nicols). FIG. 27 (middle right). (W.A.M. 12297 u): mesostasis of pigeonite (grey), tridymite (white), and magnetite (black) in a coarsely ophitic eucrite enclave. The large white crystal is bytownite and the grey euhedral grains enclosing it are pigeonite

followed much the same course as in enclave F described above, but feldspar and pyroxene seem to have come out together. A trace of pyroxene–tridymite mesostasis is evident, but nowhere near as abundant as in enclave U (below).

Enclave K shows an alternation of *ophitic* and *sub-ophitic* texture. The plagioclase was determined optically as An_{75} (bytownite). It is particularly full of inclusions, many of which yield bright second-order polarization colours. Once again there is limited development of pigeonite–tridymite mesostasis. The mode is: Bytownite $45\frac{1}{2}$ vol. %, pigeonite $46\frac{1}{2}$, tridymite 5, magnetite 3.

Enclave U is characterized by an extensive development of fine pigeonite–tridymite intergrowth as a mesostasis (fig. 27), which occupies more than one-third of the area of the thin section. Two generations are present (one maximum tridymite grain length 30 mm: the second maximum tridymite grain length 15 mm). In the mesostasis the tridymite forms small, evenly spaced, decussate laths, separated by rounded grains of pyroxene and a little magnetite in similar sized grains (as in fig. 29). The main crystallization of this enclave is more coarse than those so far described, feldspars (An_{77}) up to 2 mm long interdigitating with substantial pigeonite grains. Again fine cracks traverse the enclave, widening here and there into droplet-like swellings infilled with an opaque substance (iron oxides after nickel-iron). Similar deposition has occurred along grain boundaries, which seem to have been opening up. The mode is: Bytownite 37 vol. %, pigeonite $42\frac{1}{2}$, tridymite 17, magnetite $3\frac{1}{2}$.

The texture of enclave U is reminiscent of quartz dolerite from terrestrial dykes, for these often show ophitic texture and substantial interstitial development of quartz–feldspar mesostasis, which may locally cover a substantial area of the thin section. Such development is patchy in quartz dolerites and a comparable patchy development of abundant mesostasis in the eucrite is suggested here. The plagioclase and pyroxene appear to have come out together, followed by tridymite and then

---

(×11; plane polarized light). FIG. 28 (bottom left). (W.A.M. 12297 x): An enlargement of a similar mesostasis showing tridymite (white laths), pigeonite (grey), and magnetite (black) inset in a coarse aggregate of bytownite (riddled with droplet inclusions), pyroxene (light grey) and magnetite (black) (×27; plane polarized light). FIG. 29 (bottom right). (W.A.M. 12297 jj): A sub-ophitic intergranular textured eucrite enclave showing unusually long, thin bytownite laths (twinned) enclosing pyroxene aggregates, which have locally been comminuted, producing areas not unlike the finely brecciated material of the mesosiderite (host ×27; crossed nicols).

magnetite. Two periods of mesostasis crystallization were succeeded by brecciation, veining, and nickel-iron invasion.

Enclave X is similar, except for the attenuation and length of the bytownite laths (up to 41 mm) and the lack of twofold character to the mesostasis (fig. 28). The mode is: Bytownite 30 vol. %, pigeonite 53, tridymite 13, magnetite 4.

Enclave D (fig. 26) shows a transition from sub-ophitic to granulitic texture—the plagioclase crystals are broad and mostly without much elongation, and they, together with the pyroxenes, are mostly anhedral. The feldspar is bytownite: the grains are rather larger than the pyroxene grains, and some digitation is evident. There is a generation of smaller grains, amongst which tridymite snd magnetite are prominent, filling interstices and forming narrow stringers along the grain boundaries. The pyroxene is all pigeonite, showing low optic angles ($2V \sim 0$), but there is zonation, roughly concentric or irregular, into areas of lower and higher birefringence. The pyroxene is dusted with small inclusions along the exsolution lamellae. The mode is: Bytownite 51 vol. %, pigeonite 41, tridymite 7, magnetite 1.

Plagioclase apparently came out just before pigeonite, tridymite and then magnetite coming out with the last crystallization of the two essential minerals as a mesostasis.

Enclave H (fig. 23) shows the most perfect of the granulitic eucrite textures yet recognized. The mosaic of rounded, anhedral grains of bytownite, pigeonite, and tridymite (there is no ore mineral in the slide), and the uncomplicated sutures provide a texture that is not, like the ophitic and sub-ophitic textures described above, entirely typical of terrestrial doleritic and gabbroic rocks, for, though such textures do occur in layered gabbro intrusions, they are more typical of granulitic metamorphic rocks. The tridymite is mainly confined to fine interstitial aggregates, which apparently represent a late-stage mesostasis. The texture is not unlike an intercumulus such as is found in convective suites of noritic and gabbroic igneous rocks.

The pyroxene is zoned and in this thin section hypersthene is present, showing birefringent augite exsolution lamellae $\parallel$ to (100) standing out against a grey background of low birefringence under crossed nicols, as well as varieties of pigeonite. The hypersthene is biaxial negative and the optic angle moderate ($2V \sim 60°$) in contrast to that of the pigeonite (2V 0 to 20°); traces of earlier exsolution lamellae of the pigeonite parallel to (001) cross the exsolution lamellae of the hypersthene, suggesting inversion from pigeonite, and this is further suggested

by the fact that pigeonite is generally peripherally enclosed by hypersthene. The feldspars (An_{75}) are quite clear—devoid of inclusions—but while some grains show good cleavage others are markedly free from cleavage. The mode is: Bytownite 46 vol. %, pigeonite 40, tridymite 14. The order of development was plagioclase coming out just before the pigeonite, which became unstable and was converted to hypersthene; tridymite came out late. The sequence is similar to that seen in the unequivocably magmatic ophitic and sub-ophitic eucrite enclaves.

Enclave Z shows long narrow plagioclase laths forming an ophitic texture (fig. 20).[1] The feldspars seem strained, the twin lamellae being indistinct. Limited recrystallization of the pigeonite to aggregates of smaller grains is seen. These are of the same mineral—there is no metamorphism involved. This feature marks an incipient development of shock granulation, seen fully developed in enclaves J and W (below).

In contrast to enclaves J and W it is the pyroxene grains and not the feldspars that are strongly granulated. The attenuated laths of tridymite traverse granulated areas of the pyroxene quite unaffected. The secondary generation of pigeonite grains even displays the fine exsolution lamellae characterizing the primary pigeonite in all these eucrite enclaves. Very pronounced development of spindle-like droplet inclusions in the feldspars may or may not be related to the granulation—the juxtaposition may be fortuitous. The mode is: Bytownite 33 vol. %, pigeonite 59, tridymite 4, magnetite 4.

Enclave C_3, characterized by a sub-ophitic intergranular texture and even more attenuated feldspar laths, shows slightly more advanced granulation. The pyroxenes are mainly affected but the borders of the feldspars are frayed. The finely granulated patches are cloudy and riddled with opaque ore minerals in the form of fine specks—and these are, at least in part, of nickel-iron. These areas are not unlike the breccia zones seen in the brecciated eucrite (below).

Enclave W shows complete granulation of the feldspars. The ophitic texture is still preserved but the clear-cut feldspar laths have been converted to an aggregate of rounded granules, which, however, show polysynthetic twinning in some instances, though most are untwinned. The outlines of the feldspar laths have become ragged. The other minerals are slightly granulated, but substantial cores of the primary pigeonite grains remain.

Enclave J, the large enclave shown in figs. 5 and 8, shows comparable granulation. However, in this case the tridymite has been granulated

[1] This enclave was analysed (see Table I).

like the feldspar, forming rounded pools. The pigeonite is only partly granulated. This granulation represents a cataclasis without metamorphism—there has been no chemical or mineralogical change accompanying the mechanical deformation. Its nearest analogues are certain *flaser gabbros* (for example the gabbro from Penig, Saxony—Krantz, undated, specimen 84). Similar effects are not uncommon, also, in terrestrial anorthosites. When seen in terrestrial rocks such effects are usually taken to indicate protoclastic deformation, superimposed without thermal effects in such a manner as not even to destroy the primary pattern—a form of cold cataclasis without strong directed pressure.

Brecciated eucrite enclaves

While the 'shocked', ophitic-textured eucrite enclaves described above are not, strictly speaking, brecciated, but have suffered granulation and recrystallization to a finer crystalline aggregate, there are evidences of brecciation in most of the eucrite enclaves, though these are mostly slight, and take the form of a network of hair-line cracks infilled with nickel-iron specks and troilite or ferruginous oxides derived from these minerals.

However, *enclave V* shows a distinct zone of brecciation, characterized by fine crush, angular clastic fragments derived from the crystals of the eucrite, and nickel-iron penetration. The unbrecciated material in this eucrite enclave is very coarsely ophitic and in no way unusual (fig. 25), though the tridymite is crystallized in a distinct rounded pool of finely granular mesostasis (*cf.* the shocked eucrite enclave J described above). This unbrecciated material displays a sharp contact (fig. 25) against alternating bands of finer, granular material, not entirely brecciated but including bands of fine crush virtually free of metal and inset with broken fragments of larger crystals. One of the finely granular bands displays numerous small specks of nickel-iron.

It seems reasonable to deduce that, with the incoming of the nickel-iron, there was considerable 'shock' deformation experienced by the existing achondritic material. The effect of this was, in the first place, granulation without chemical or mineralogical change, but this was superseded by brecciation characterized by the formation of fine crush and broken crystals separated from the achondrite enclaves. The nickel-iron mainly followed the paths supplied by the tracery of fractures formed in the brecciation phase, but in enclave V seems to have preferentially penetrated a layer of finely granulated material. While the granulation that produced the 'shocked' eucrite enclaves shows no

evidence of having been due to a directed stress, the lamination of the granulation and brecciation zones in enclave V does suggest some form of directed stress. However, these contrasting layers could have stemmed in the first place from a primary set of contrasted bands in the original enclave (bands analogous to magmatic layering in gabbroic rocks from lopoliths), and the brecciation zones could have simply developed along these earlier formed bands.

The brecciation seen in enclave V is not unlike the effect seen in small areas of enclave C_3 (described above): one cannot escape the conclusion that 'shock granulation', brecciation, and invasion by nickel-iron to form the predominant reticulated, metalliferous host material, all represent phases in one process. While one cannot be sure of the time relationship between these phases, they may have occurred within a short period in the history of the parent body. The time interval between these secondary processes and the initial magmatic crystallization may have been short or lengthy, but because specks of nickel-iron seem to be aggregated in the end-phase ore mineral of the eucrites, it is not beyond the bounds of possibility that the sequence was almost continuous and that the metallic invasion and brecciation formed part of the late phase crystallization—for there is difficulty in enclave C_3 in separating end-phase mesostasis from areas of secondary granulation, a fact that may mean much or little.

The hypersthene achondrite inclusions

Inclusion T, being an angular enclave of similar appearance, was at first thought to be an eucrite enclave. Thin section study revealed a quite different material (fig. 31); there is no feldspar present and the rock is virtually monomineralic; though the dominant ferro-magnesian mineral is not unlike the olivine of the olivine achondrites in appearance (*cf.* figs. 17 and 32), the texture is much finer and the hypersthene could be distinguished on account of its lower birefringence and more perfect cleavage, and also on account of the negative optical sign. The only other minerals present are minor accessories—specks of tridymite and a birefringent clinopyroxene interstitial to the hypersthene aggregate, and magnetite occurring as sparse and minute specks. A mineral present as minute needles appears to be apatite. This material is in no way dissimilar to the rare, virtually monomineralic, calcium-poor achondrites, the *hypersthene achondrites* or *diogenites* (Mason, 1963).

The texture is not conspicuously brecciated, though some of the original hypersthene grains have been granulated to form fine interstitial

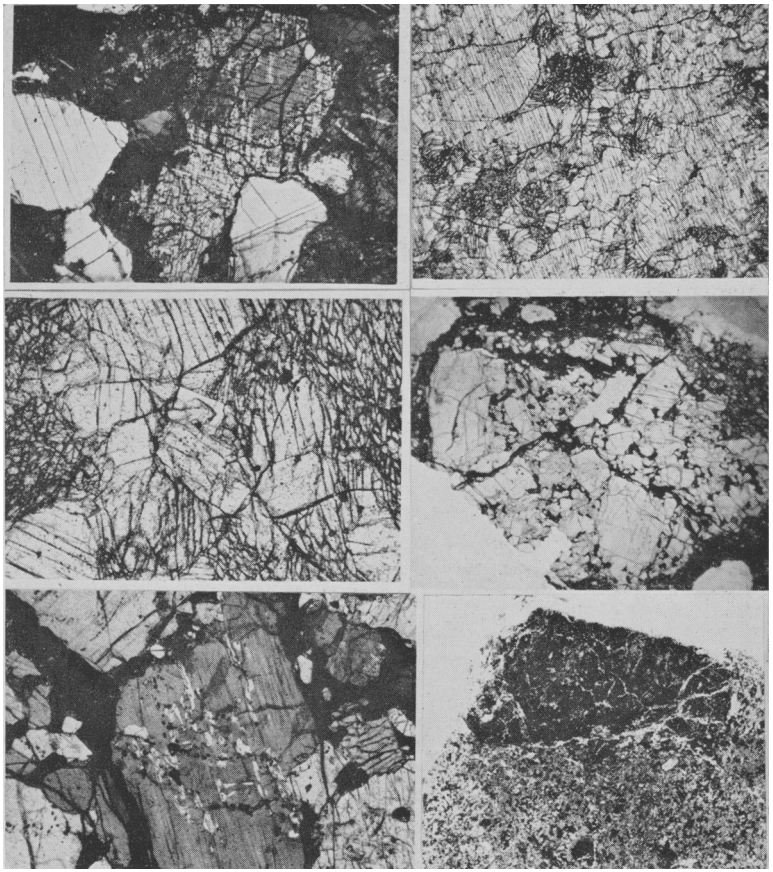

FIGS. 30–35: FIG. 30 (top left). (W.A.M. 12297 r): Showing pigeonite cores (medium grey) enclosed by hypersthene (light grey). The latter mineral shows lamellar exsolution of clinopyroxene parallel to (100) (×30, crossed nicols). FIG. 31 (top right). (W.A.M. 12297 t): Hypersthene achondrite (diogenite) enclave showing the remains of a medium-coarse, granulitic texture, partly obliterated by intergranular comminution. The cleavage of the pyroxene grains (the only mineral present is hypersthene) is rather more finely ruled than in the case of the olivines (*cf.* Figs. 17 and 18) (×12; plane polarized light). FIG. 32 (middle left). (W.A.M. 12297 v): The same, enlarged, showing the cleaved, uncomminuted relict hypersthene grains and one single intergranular grain of tridymite (white) (×47; plane polarized light). FIG. 33 (middle right). (W.A.M. 12297 aa): An unusual lithic enclave set in the metalliferous host (dark, fringing material). The enclave consists of an intergrowth of anhedral-subhedral grains of pyroxene, resembling hypersthene but showing markedly oblique extinction (×5; plane polarized light). FIG. 34 (bottom left). (W.A.M. 12297 aa): One of the grains in the above photomicrograph viewed

aggregates—a structure resembling that seen in the olivine achondrite enclaves (p. 1040). The presence of larger crystal remnants of hypersthene (up to 8 mm long) show that this material was formerly more coarsely crystalline compared with its present state.

The hypersthene is non-pleochroic and its composition is Fs_{25} (refractive index determination, by Mason), a value typical of the diogenites and also, significantly, close to the value obtained for hypersthene in the host material. The included clinopyroxene shows second-order polarization colours, contrasting with the low birefringence of the hypersthene: the extinction angle is up to 38°, and 2V about 60°. These grains are, however, too small for the species of clinopyroxene to be identified, though diopside seems more likely than pigeonite. The tridymite (fig. 32) is of the mottled variety seen in the eucrite enclaves: its mean refractive index is 1·472 (birefringence 0·003): its presence suggests a genetic connexion between diogenite and eucrite—both may have stemmed from magmatic crystallization, the diogenite coming from an area of the melt of slightly different composition. The occurrence of diogenite may well be related to the end-stage production of hypersthene from pigeonite seen in one eucrite enclave (H), significantly a granulitic eucrite enclave with a texture not unlike that of this diogenite enclave. The occurrence of tridymite in this enclave and that eucrite enclave is similar—it suggests an intercumulus crystallization.

The ore mineral in the diogenite was identified as magnetite on account of its reflectance, but some nickel iron may also be present. Another *enclave, C*1, proved to be entirely similar except for rather more abundant tridymite. These enclaves are rare and of small size compared with the eucrite enclaves.

Another *enclave, E*, seen only within a thin section of the host material (figs. 33 and 34), is entirely composed of pyroxene, but though of low birefringence the pyroxene shows markedly inclined extinction (up to 26°), and 2V $\sim 60°$. This mineral encloses many irregular flecks of birefringent clinopyroxene and there is also evident a fine, faint lamination under crossed nicols, the laminae having spindle form and being

---

under higher power and crossed nicols. The lenticular lamellation and ragged specks of more birefringent clinopyroxene (due to exsolution) are clearly seen ($\times 30$; crossed nicols). FIG. 35 (bottom right). Olivine enclave within mesosiderite host material: not only the large enclave is composed entirely of olivine, but the nearby smaller enclaves are similarly composed, clearly indicating invasion and fragmentation of a larger, continuous olivine mass by nickel-iron. (Specimen 6252, School of Mines, Kalgoorlie, collection.)

parallel to the elongation (*cf.* G. J. H. McCall, *The Frenchman Bay Meteorite*, Journ. Roy. Soc. Western Aust., *in the press*, for description of similar pyroxenes in a chondrite meteorite).[1] The optical properties are those of hypersthene but for the oblique extinction. Similar lamellar clinopyroxenes in chondrites are being investigated by Dr. B. H. Mason at the present time and a fuller explanation of this phenomenon may be expected.

TABLE I. Chemical analyses of the Mount Padbury mesosiderite

	1.	2.	3.	4.			2*a*.	3*a*.
SiO_2	20·67	20·67	47·50	53·23	Tridymite		—	1·37
TiO_2	0·30	0·30	0·68	0·27		Or		0·20
Al_2O_3	3·93	3·93	13·00	0·87	Feldspar	Ab	10·75	4·45
Cr_2O_3	0·30	0·30	0·43	0·84		An		33·02
FeO	—	5·36	20·50	17·14		Wo		6·61
MnO	0·20	0·20	0·57	0·60	Diopside	En	29·0§	2·14
MgO	7·73	7·73	6·49	25·92		Fs		4·69
CaO	2·17	2·17	9·85	1·16	Hypersthene	En		14·03
Na_2O	0·12	0·12	0·53	—		Fs		29·54
K_2O	0·02	0·02	0·03	—	Ilmenite		—	1·35
P_2O_5	0·11	0·11	Nil	—	Chromite		0·5	0·63
C	0·70	0·70	—	—	Troilite		7·5	1·10
S	2·69	7·37†	0·40	—	Graphite		0·7	—
Fe	51·33*	36·77	—	—	Metal		42‖	—
Ni	5·06	5·06	—	—	Limonite		9·75	—
Co	0·16	0·16	—	—				
H_2O†	0·92	—	0·10	—				
FeO.OH	—	9·07	—	—				
Sum		100·04	100·18‡	100·06				

1. Mesosiderite host material, somewhat rusted. Anal. H. B. Wiik.
2. Anal. 1 recalculated to fit the mineralogy.
2*a*. Norm of the mesosiderite host material.
3. Eucrite enclave Z. Anal. A. A. Moss.
3*a*. Norm of eucrite enclave Z.
4. Hypersthene from diogenite enclave T. Anal. H. B. Wiik. Optics: α 1·686, γ 1·698 (Na), B. Mason. Composition Fs 27 mol. % (anal.), 28 (opt.).

* Total iron as metal. † FeS. ‡ Including 0·30 H_2O^- and less 0·20 for S.
§ MgO/FeO 3. ‖ Fe/Ni 8·5.

Chemical analyses

The sample of mesosiderite host material analysed (table I, cols. 1, 2, and 2*a*) was free from any substantial achondrite inclusions, but the metal had been partly oxidized to goethite. Assuming that no nickel has been lost during this oxidation and that the silicate is wholly plagioclase and hypersthene with Fs 28 mol. %, the iron can be allotted as shown in col. 2. Though there are some olivine and some pigeonite present, the errors introduced would act in opposite directions. The total silica

[1] Mason (written communication) suggests that they are clino-hypersthene.

required for plagioclase and pyroxene on this basis is 21·1 %, in good agreement with the observed 20·67 %.

If no nickel has been lost, the composition of the metal must have been near 11·9 % Ni. The allocation of iron to metal and limonite has been made on the assumption that all H_2O found is present as FeO.OH; since there is likely to be considerable adsorbed water, the amount of limonite is probably overestimated. The analysis and norm of the host material agree closely with those of Hainholz (Prior, 1918).

One of the eucrite enclaves (Z) was also analysed (table I, cols. 3 and 3*a*), and compares well with the average of 13 eucrite analyses (Wood, 1963). No analysis of a diogenite enclave was attempted, but hypersthene was separated from enclave T and gave the results shown in table I, col. 4.

Discussion

This detailed petrographic study suggests that olivine achondrite, eucrite ('basaltic achondrite') and hypersthene achondrite ('diogenite') material has initially crystallized slowly and under somewhat raised temperatures compared with terrestrial igneous rocks. The slowness of the cooling is reflected in characteristically 'plutonic' crystallinity of texture, and also in the presence of regular augite exsolution lamellae within the pigeonite of the eucrite: for this exsolution phenomenon is reportedly only developed in slow-cooled magnesian pigeonites, just prior to inversion to hypersthene (Deer, Howie, and Zussman, 1963, p. 148–149). The presence of tridymite rather than quartz suggests somewhat raised temperatures, since this is the form of silica stable at moderately high temperatures (876 to 1473° C), but the exact nature of the factors controlling the development of the major polymorphs of silica are obscure. The presence of tridymite does indicate a pressure of less than 3000 Kg/cm (Mason, 1962, p. 68).

That this patchy, inhomogeneous silicate mass stemmed from a cooling melt or *magma* cannot be doubted: one cannot conceivably produce ophitic, sub-ophitic, and intergranular textures such as are evinced by the eucrite in any other way. The diogenite contains the same late tridymite phase as the eucrite, so one may reasonably infer that it, too, is of magmatic origin. The olivine crystals are of considerable stature, far exceeding any other mineral of the silicate aggregate, and, although there is no firm evidence of magmatic crystallization in this case, the evidence of large phenocrysts in howardite from Dalgaranga (McCall, 1965, p. 480) and Dingo Pup Donga (McCall, unpublished results on

a new howardite find in Western Australia) suggests that these may be early crystallizations of phenocryst stature—though the excess tridymite of the eucrite, incompatible with olivine, suggests disequilibrium conditions. The olivine is unquestionably present in the form of residual enclaves within the metal tracery (fig. 35), like the eucrite.

The next event seems to have been granulation, without any concomitant metamorphism, of part of the early formed silicate: this was accompanied by limited brecciation and veining. At the same time the two non-silicate fractions (presumably initial immiscible fractions produced during melting subsequent to accretion) invaded the mechanically altered silicate mass, entering the granulated and brecciated areas preferentially. The sulphide fraction seems to be restricted to a fine interlacing of the silicate areas, which form reticulations within the network of nickel-iron. It is probable that the nickel-iron crystallized first and the sulphide later—the brittle nature of the silicates encouraging preferential troilite penetration. The crystallization of the nickel-iron was sufficiently slow for Widmanstätten figures, such as are typical of medium octahedrites of the same composition, to be formed in the larger nodular expanses of metal.

If we take into consideration the fact that the oxides, ore minerals, and nickel-iron seem to show very sparse distribution within the silicate fraction, and that these specks seem, in many cases, to be primary and not late invasions, it appears that the metal and sulphide phases followed reasonably quickly on the silicate crystallization. These three phases are of course Goldschmidt's primary differentiates, not miscible under any conditions, and responsible for the primary separation of the lithophile, siderophile, and chalcophile element associations that govern the geochemical distribution of elements in our planet (Ahrens, 1965). Beyond this there is a pattern of successive crystallization that has considerable relation to melting-points. The sequence of development of this meteoritic material in the parent body may be represented, with time running from left to right, and with granulation, brecciation, and the introduction of the siderophile and chalcophile phases at the breaks shown:

Lithophile	*Siderophile*	*Chalcophile*
Olivine		
Pigeonite Hypersthene		
Plagioclase		
Tridymite		
Magnetite	Nickel-iron	Troilite

The olivine achondrite, eucrite, and diogenite material is shown above in sequential relationship, in terms of time and slowly falling temperature: however, this is only one alternative interpretation of the diogenite, as a residual crystallization—a late stable mineralogical assemblage formed subsequent to the eucrite material.

Against this interpretation it must be noted that the hypersthene examined is less iron-rich than the pigeonite, and fractional crystallization of pyroxenes always proceeds towards the iron-rich end of the isomorphous series. Thus one may well doubt whether the hypersthene developed in coronas around the pigeonite corresponds to that of the diogenite in composition, and prefer to interpret the diogenite as simply representing chemically contrasting areas in the inhomogeneous mass, areas of crystals separated out between the olivine and the eucrite.

In this case the sequence should be represented as:

Olivine
Hypersthene
Pigeonite → Hypersthene

The presence of coronas indicates disequilibrium conditions, and this is also suggested by the co-existence of olivine and tridymite in the silicate mass. Surprisingly this patchily inhomogeneous mass of silicate crystals seems to have only established homogeneous equilibrium over very restricted areas as the temperature continued to fall. An alternative explanation would be that the olivine and eucrite are unrelated fragments—yet the systematic character of mesosiderite mineralogy (McCall, 1965*b*, p. 484) suggests that this is not the answer.

The further inference that may be drawn from this study is that the calcium-poor achondrites are not simply the products of transformation of chondrites—they are probably best regarded as direct products of crystallization from a primary melt, subsequent to accretion, and representative of a different part of the parental planetary body.

Though we have, in the Mount Padbury meteorite, a discrete 600 lb mass (though broken into fragments by various terrestrial agencies), we are seeing, in reality, the stages in solidification of a mantle (main silicate layer), and in all probability the deeper part, close to the metal core (assuming that a core existed, for iron meteorites may only represent patches in the lower part of an inhomogeneous mantle of a coreless parental planetary body). The fact that Widmanstätten patterns are present within nodules of nickel-iron in this meteorite favours the model of Fish, Goles, and Anders (1960) rather than the popular concept of Phaeton in which basaltic achondrite material is referred to the crust.

No-one has ever suggested that Widmanstätten patterns—never produced in the laboratory on anything but a microscopic scale—could form without very prolonged crystallization conditions, such as could only pertain within a planetary interior, and if the nickel-iron crystallized under such conditions, then so must the eucrite. Intense pressures are no longer considered essential to form these patterns and the presence of tridymite indeed seems to preclude very great pressures

This pressure restriction appears to favour a small parental body rather than a large one. Opinions differ on this point—asteroidal, lunar, and earth-sized planetary bodies have been postulated by different authors for the meteoritic parent—but it must be recorded that the eucritic material is extraordinarily terrestrial in appearance, and that Hess and Henderson (1949) have brought forward petrofabric evidence for crystallization in a gravitational field like that of the Earth in the case of the very similar Moore County eucrite. Could an asteroid of the size of Ceres conceivably exhibit such astonishingly terrestrial crystallization in its interior?

Of course it could be suggested that the Mt. Padbury meteorite is nothing but part of one of the primary objects of lunar size postulated by Urey (1959) and supposed to consist of achondrite material and stony iron material. But the evolutionary picture deduced from this study; the lack of diversity of mineral species as reflected in fayalite and ferrosilite indices (the only variation seen is in the pigeonite and plagioclase and this is compatible with slight temperature variation or compositional inhomogeneity during cooling); the lack of diversity of the achondrite types, two out of the three certainly being genetically related; the chemical and mineralogical unity of the mesosiderite group as a whole (McCall, 1965, Table 1, p. 484) just cannot be reconciled with this idea, already discounted by the evidence of chondrite inclusions in the Bencubbin meteorite (Lovering, 1962), and we cannot longer be concerned with it here. There may be many unresolved anomalies but this inhomogeneous meteorite mass must surely represent the product of cooling in the interior of a planetary body of an association of three immiscible liquids, solidifying one after another, and suffering some localized granulation and brecciation in the later stages of solidification.

The parent planet or asteroid was fragmented by some cause unknown and this material was hurled into an elliptical orbit, and by chance one that was likely to bring it eventually into earth collision. It is worth bearing in mind the number of such masses which must have been hurled out without any such possibility—the meteorites we receive represent

a small, select minority of asteroidal material and may not be at all representative either in type ratios or in over-all composition. After many millions of years in orbit this collision occurred, and it plunged momentarily through the atmosphere, being ablated at the surface, fragmenting in flight, suffering secondary ablation, and further fragmentation on impact. Many years, possibly thousands of years, of sojourn on the ground, the material being once more fragmented and covered with an oxide skin by weathering agencies, probably followed: until a chance traveller searching for his sheep remarked it and yielded it to mankind for scientific study.

The study of this unique meteorite is only beginning. Much detailed geochemical and physical study must follow in the near future. The material is held at the School of Mines, Kalgoorlie, and the Western Australian Museum, and the issue of material for further specialized study will be decided upon by the Head of the Geology Department at the School of Mines and the Meteorite Advisory Committee of the Museum, working in close consultation.

Acknowledgements. The author is indebted to the finder Mr. W. C. Martin and to Mr. W. H. Cleverly who recovered the material: the latter gave him much assistance in selecting material for study. Dr. B. Mason assisted him with mineralogical determinations and in many other ways; he also read the draft manuscript critically, suggesting several improvements. Others who assisted the writer are Mr. J. R. de Laeter (X-ray diffraction studies), Mr. N. J. Stephenson (confirming mineralogical determinations) and Mr. W. Smeed (who prepared numerous excellent thin and polished sections, which provide the basis for this petrographic study). Mr. K. C. Hughes was responsible for preparing the photographic illustrations.

References

AHRENS (L. H.), 1965. Distribution of the Elements in Our Planet. New York (McGraw Hill).

CLEVERLY (W. H.), 1965. Journ. Roy. Soc. Western Australia, vol. 48, pp. 45–49.

DEER (W. A.), HOWIE (R. A.), and ZUSSMAN (J.), 1963. Rock Forming Minerals, London (Longmans).

FISH (R. A.), GOLES (G. G.), and ANDERS (E.), 1960. Astrophys. Journ., vol. 132, pp. 242–58.

HESS (H. H.) and HENDERSON (E. P.), 1949. Amer. Min., vol. 34, pp. 494–507.

KRANTZ (F.). Description of the Rocks (privately printed handbook issued with a rock specimen collection).

KRINOV (E. L.) [Кринов (Е. Л.)], 1961. Principles of Meteoritics. New York (Pergamon). Translation of Основы Метеоритики

LOVERING (J.), 1962, in Researches on Meteorites (edit. C. B. Moore), pp. 179–198. New York (John Wiley).

MCCALL (G. J. H.), 1965*a*. Meteoritics, vol. 2, pp. 315–323.

—— 1965*b*. Min. Mag., vol. 35, pp. 476–487.

—— and DE LAETER (J. R.), 1965. Catalogue of Western Australian Meteorite Collections. Spec. Publ. no. 3, Western Australian Museum.

McCall and Cleverly (W. H.), 1965. Nature, vol. 207, pp. 851–852.
Mason (B.), 1962. Meteorites. New York (John Wiley).
—— 1963. Amer. Mus. Novitates, no. 2155.
Nininger (H. H.) and Huss (G. I.), 1960. Min. Mag., vol. 33, pp. 619–639.
Prior (G. T.), 1918. *Ibid.*, vol. 18, pp. 151–172.
Urey (H. C.), 1959. Journ. Geophys. Res., vol. 64, pp. 1721–1737.
Winchell (A. N.) and Winchell (H.), 1951. Elements of Optical Mineralogy, 4th edn, pt. 2. New York (John Wiley).
Wood (J. A.), 1963, in The Moon, Meteorites and Comets, pp. 337–401, ed. B. M. Middlehurst and G. P. Kuiper. (Univ. Chicago Press.)
Yoder (H. S.) and Sahama (Th. G.), 1957. Amer. Min., vol. 42, pp. 475–491.

[*Manuscript received 2 June 1966.*]